JOURNAL OF PROPULSION AND POWER
Vol. 18, No. 6, November–December 2002

Effects of Blade Count on Linearized and Nonlinear Hot Streak Clocking Simulations

Douglas L. Sondak*
Boston University, Boston, Massachusetts 02215
Vipul Gupta† and Paul D. Orkwis‡
University of Cincinnati, Cincinnati, Ohio 45221-0070
and
Daniel J. Dorney§
NASA Marshall Space Flight Center, Marshall Space Flight Center, Alabama 35812

The temperature field exiting gas turbine combustors is highly nonuniform due to streaks of hot fluid directly downstream of combustor fuel nozzles. These hot streaks have been shown to limit the life of turbine blades. Adjusting the positions of hot streaks with respect to nozzle guide vanes, known as hot streak clocking, can be used to help control blade temperatures in gas turbines. Because hot streak clocking predictions require unsteady, three-dimensional simulations, they are very expensive, and various techniques are used to reduce their cost. Two of these techiques are examined, linearized Navier–Stokes solvers and reduced-blade-count simulations. Hot streak clocking simulations have been performed using nonlinear and linearized Navier–Stokes solvers for 1–1–1 and 3–4–3 blade-count (blades per row) configurations. The blade-count effects were examined for each solution technique, and the two solution techniques were compared. It is shown that the linearized technique can be used to capture qualitatively hot streak clocking effects. It is also shown that the reduced-blade-count approximation has a significant impact on predicted surface temperatures.

Nomenclature

C_p = $(P - P_{\text{exit}})/(P_{t\infty} - P_{\text{exit}})$
P = pressure
T = temperature
β = flow angle, deg

Subscripts

t = total
∞ = inlet

Introduction

IN jet engine combustors, fuel is introduced through nozzles at a number of circumferential locations. As combustion occurs, the flow downstream of the nozzles is hotter than the surrounding fluid,[1] a phenomenon known as hot streaks. The hot streaks maintain their identities as the flow convects through the vanes of the high-pressure turbine, and the turbine rotor blades operate in the presence of an unsteady inlet temperature field. As hot streaks interact with the rotor blades, they can cause localized hot spots on the blade surfaces, leading to diminished blade life, or in the worst case to blade failure.

An early experimental investigation of hot streak migration was performed by Butler et al.[2] They showed that hot streaks cause increased temperature on rotor blade pressure surfaces and decreased temperature on suction surfaces. The temperature patterns were attributed to two effects: changes in secondary flow patterns due to presence of the hot streaks and circumferentially varying inlet relative flow angle, as discussed by Kerrebrock and Mikolajczak.[3] They also verified the analysis of Munk and Prim,[4] showing that the hot streak will not migrate as it convects through the vane.

Krouthén and Giles[5] performed a two-dimensional simulation based on the Butler et al.[2] experiment. They found discrepancies between the experimental and computational results, which they attributed to the importance of three-dimensional effects. Their conclusion was verified by Dorney et al.,[6] who performed two-dimensional and three-dimensional simulations based on the same experiment. Their three-dimensional results showed a better match with experimental time-averaged midspan rotor surface temperature than the two-dimensional results.

In addition to secondary flow and circumferentially varying relative inlet angle effects, Shang and Epstein[7] showed that hot streak migration is also affected by buoyancy, which tends to drive the hot streak toward the hub. Their inviscid simulations also showed that the rotor blade surface temperature distribution is affected by the number of rotor blades given a fixed number of vanes.

It has been demonstrated that blade temperatures can be modified by adjusting the circumferential locations of the stationary blades with respect to the combustor hot streaks, known as hot streak clocking.[8–11] Turbine rotor blade temperatures can be decreased significantly by aligning the hot streaks so they impinge on the nozzle guide vane (NGV) blades. Because NGV blades are typically designed to handle stoichiometric temperatures, they can withstand the higher temperatures due to hot streak impingement.

Because hot streak clocking has a large effect on turbine rotor blade temperature distributions, and these temperatures are of critical importance to the structural integrity of the blades, it is important for designers to predict these effects. Unfortunately, as already discussed, this requires unsteady, three-dimensional flow simulations, and these are far too time consuming to be of use as part of the day-to-day design process.

Two methods of reducing the computational effort in predicting blade temperatures are examined in the present study, reduced blade

Presented as Paper 2001-3476 at the AIAA 37th Joint Propulsion Conference and Exhibit, Salt Lake City, UT, 8–11 July 2001; received 28 September 2001; revision received 11 September 2002; accepted for publication 12 September 2002.

*Senior Scientific Programmer, Office of Information Technology. Senior Member AIAA.
†Graduate Student, Department of Aerospace Engineering. Student Member AIAA.
‡Associate Professor, Department of Aerospace Engineering. Senior Member AIAA.
§Aerospace Engineer, Applied Fluid Dynamics Group. Associate Fellow AIAA.

counts and linearized Navier–Stokes solvers. It is common practice to modify blade counts in unsteady, three-dimensional turbomachinery simulations to avoid the necessity of solving all of the passages in each row, but the effects of this assumption on hot streak clocking results have not been evaluated. If it could be demonstrated that reduced blade counts do not substantially degrade blade temperature predictions, this would be of significant benefit to the designer. The linearized Navier–Stokes method of Orkwis et al.[12] has shown promise for the prediction of unsteady turbomachinery flows with less computational effort than full nonlinear solutions. Here, it is compared in accuracy and efficiency to a nonlinear solver for the hot streak problem.

Benchmark solutions were first performed using a three-dimensional, unsteady Navier–Stokes solver (nonlinear) to solve the flowfield through a $1\frac{1}{2}$-stage turbine with a total of 10 passages (3–4–3). Two hot streak clocking positions were examined: impinging on the NGV and convecting midpassage through the NGV blade row. The same simulations were then performed using the linearized solver. All of these simulations were then repeated using a reduced (1–1–1) blade count. This matrix of simulations allowed the assessment of both blade-count effects and linearized-solver effects on the blade temperature distributions as compared with the benchmark solutions.

Nonlinear Navier–Stokes Solver

The three-dimensional, Reynolds-averaged, unsteady, Navier–Stokes equations were solved using an implicit, time-marching, finite difference method.[6] The inviscid fluxes were discretized using Roe's scheme,[13] and viscous fluxes were discretized using standard central differences. The Baldwin–Lomax[14] algebraic turbulence model was used for turbulence closure. The procedure is second-order accurate in time and third-order accurate in space. The equations were solved using approximate factorization and a block tridiagonal solver.

Each blade passage was modeled with an O grid around the airfoil, overset on an H grid, which fills the remainder of the passage, as shown in a typical midspan section in Fig. 1. In Fig. 1, every other grid line has been omitted for clarity. The use of overset grids permits good resolution in the leading- and trailing-edge regions and allows the application of periodic boundary conditions in the blade-to-blade direction without interpolation. The flow variables at zonal boundaries between the O grid and H grid were explicitly updated after each time step by interpolating values from the adjacent grid.

Linearized Solver with Deterministic Stresses

The time-averaged flowfield from an unsteady turbomachinery flow simulation will generally be different than the flowfield from a steady-state simulation due to nonlinear effects. Because the high computational cost of unsteady Navier–Stokes simulations limits their use in the design environment, researchers have been pursuing methods to account for some of the unsteady effects in steady-state simulations that are much less expensive. One approach is through the modeling of deterministic stresses,[15] which has been used to include some unsteady effects in steady-state simulations of blade pressure loading[16] and hot streak migration.[17] Deterministic stresses are analogous to turbulent (stochastic) stresses, but they involve deterministic timescales, such as the blade-passing time in a turbomachine. Correlation terms can be computed at these deterministic scales that are analogous to Reynolds stresses at turbulent scales.

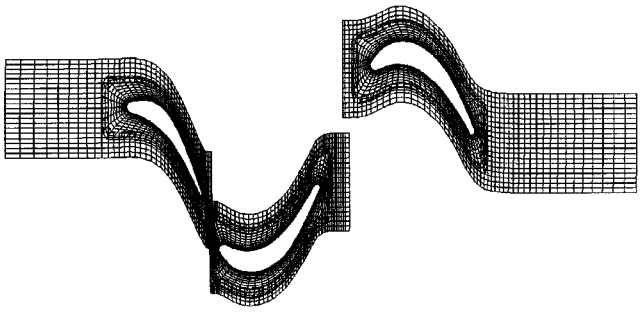

Fig. 1 Midspan section of typical grid, every other grid line.

Orkwis et al.[12] noted that linearized unsteady Euler and Navier–Stokes solvers are less expensive than unsteady Euler solvers, and they developed a method to approximate deterministic stresses using a linearized solver, which they call the deterministic source term (DST) method. A nonlinear, steady-state base case is first computed for each blade row. The unsteady flowfield is then computed using a linearized Navier–Stokes solver. Correlation terms defining the deterministic stresses are computed from the unsteady flowfield, and they are introduced as source terms in the steady-state solver, thereby including some of the unsteady effects in the steady-state solution. Orkwis et al. applied this technique to the hot streak migration problem utilizing the linearized Euler solver of Holmes et al.[18] and showed that the method is effective at capturing significant aspects of hot streak migration. In the present study, this method is extended to use a linearized Navier–Stokes solver to determine its effectiveness at modeling blade-count effects on hot streak migration and to compare its efficiency with that of the full nonlinear solver. The linearized Navier–Stokes solver is second-order accurate in space.

Configuration

The three-dimensional turbine model is based on the large-scale rotating rig (LSRR) geometry used in experiments performed by Dring et al.[19] at United Technologies Research Center. The LSRR is a $1\frac{1}{2}$-stage high-pressure turbine with a 68.58-cm (27-in.) midspan radius, 15.24-cm (6-in.) span, and airfoil aspect ratios of approximately unity. The turbine hub and casing are at constant radii. The axial gap between the first-stage stator and rotor is approximately 15% rotor axial chord, while the gap between the rotor and the second-stage stator is approximately 50% rotor axial chord. The rotor tip clearance in the experimental rig is approximately 1% of span. In the experiments, the inlet Mach number to the first-stage stator was 0.07 (with flow coefficient of $\phi = 0.78$), and the inlet flow was assumed to be axial. The rotor rotational speed was 410 rpm. The freestream Reynolds number was 3.937×10^4/cm (1×10^5/in.). The ratio of exit static pressure to inlet total pressure at midspan was 0.9505.

The experimental configuration had 22 airfoils in the first-stage stator row and 28 airfoils in each of the rotor and second-stage stator rows. To simulate this exact airfoil count, it would be required to model 11, 14, and 14 passages in the three blade rows, respectively. For one set of simulations, the first blade row was modeled as having 21 airfoils, and so the first-row geometry was scaled by 22/21 to maintain the correct blockage. In a similar fashion, the second and third blade row geometries were scaled by 28/21. This resulted in a blade count of 21–21–21 for the three blade rows, which can be modeled with one passage per row (1–1–1). For the second blade count, the first row geometry was scaled by 22/21 and the third row geometry was scaled by 28/21 to simulate a blade count of 21–28–21 (3–4–3). The NGV airfoil count in the 1–1–1 case was chosen to equal that in the 3–4–3 case so that the hot streaks would introduce the same amount of energy into the domain in both cases. For the present study it was not actually necessary to scale the third blade row. This was done because the configuration is also being used in a companion study of airfoil clocking, and because the primary concern of the present study is to examine hot-streak clocking effects in the first two blade rows, the blade count in the third row is not critical. Table 1 contains a list of the simulations that have been performed. Hot streak clocking position I indicates that the hot streak impinges on the vane, and M indicates that it passes midpassage.

In a previous study[6] the nonlinear code was validated for this configuration by comparing blade surface temperatures with experimental data.[2,11]

Grids

The grid dimensions used in the nonlinear code were determined by 1) using a two-dimensional code to evaluate the grid density needed to support the axial convection of the wakes with minimal dissipation, 2) resolving the airfoil boundary layers with approximately 15 grid points, and 3) attaining average values of y^+,

Table 1 Simulation parameters

Case	Blade count	Hot streak
1	1–1–1	No
2	1–1–1	I
3	1–1–1	M
4	3–4–3	No
5	3–4–3	I
6	3–4–3	M

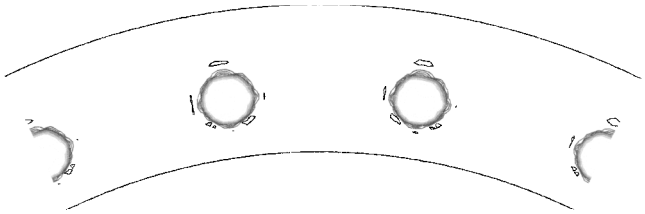

Fig. 2 Inlet temperature field, 3–4–3 blade count, contour range $0 < T/T_\infty < 1.5$.

the nondimensional distance of the first grid point above a solid wall, of approximately 1.0. The O grids were $121 \times 41 \times 53$ in the wraparound, surface-normal, and radial directions. The H grids in the first-stage stator passages were $86 \times 41 \times 53$ in the axial, circumferential, and radial directions. The H grids in the rotor and second-stage stator passages were similar, except they contained 105 points in the axial direction. Tip clearance grids were $121 \times 22 \times 9$ in the wraparound, surface-normal, and radial directions. In the 1–1–1 simulations, shown in Fig. 1, a total of 1,450,641 grid points was used. The 3–4–3 simulations contained a total of 4,861,655 points.

The linearized code used H grids rather than the overset O–H grids of the nonlinear code. The NGV grids for the nonlinear simulations were $129 \times 53 \times 53$ in the axial, circumferential, and radial directions, for a total of 362,361 points for each passage, and the rotor blade grids were $129 \times 49 \times 49$ for a total of 309,729 points for each passage. These grids resulted in values of $30 < y^+ < 150$, which was appropriate because wall functions were used.

Boundary Conditions

One hot streak with a hyperbolic tangent profile was imposed at the upstream boundary of each vane passage at 40% radius. They were circular in shape, one-third span in diameter, and had a maximum temperature 1.5 times the freestream temperature. The inlet temperature field for a case with three vane passages is shown in Fig. 2.

Characteristic boundary conditions were used at the inflow and outflow boundaries. The ratio of midspan outflow static pressure to inlet total pressure was specified as 0.9505, the experimental value, and the static pressures at other outflow radial locations were obtained from the radial equilibrium equation. Periodicity was enforced in the circumferential direction. On all solid surfaces, the no-slip condition was specified, and the normal pressure gradient was set to zero. Endwalls and airfoil surfaces were assumed to be adiabatic.

Results

Hot Streak Clocking Effects, 1–1–1 Blade Count

Experiments and simulations have shown that hot streak clocking can be used to control rotor surface temperature.[8–11] When hot streaks impinge on the leading edges of the NGVs, the rotor surface temperatures are significantly lower than cases in which the hot streaks are introduced midpassage. Simulations were performed for the 1–1–1 blade-count case using both linearized and nonlinear methods to verify that this effect is being captured and to assess the ability of the linearized method to reproduce qualitatively the nonlinear results.

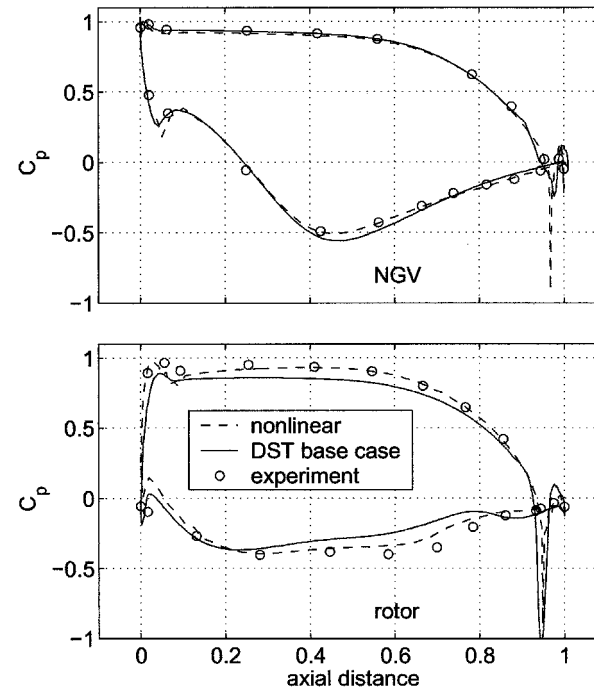

Fig. 3 Midspan pressure profiles for NGV and rotor.

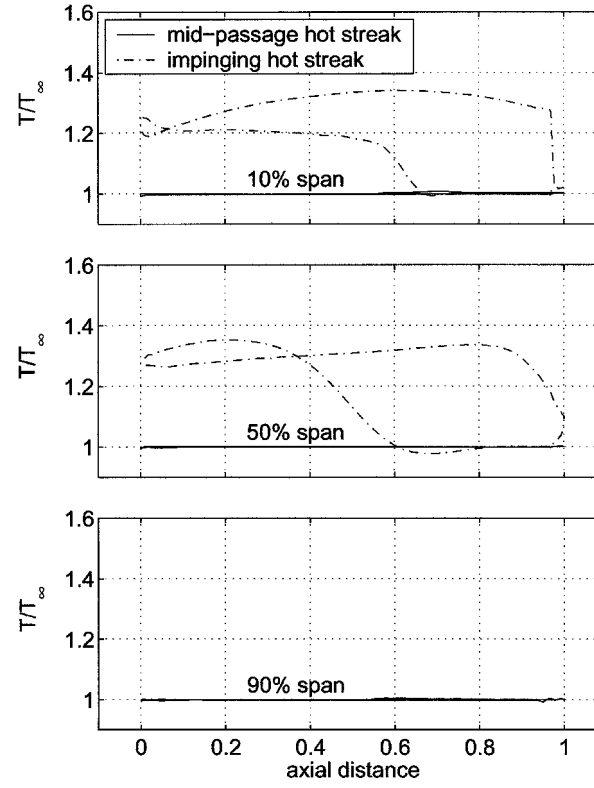

Fig. 4 Time-averaged NGV surface temperature, 1–1–1 blade count, nonlinear simulation.

Figure 3 shows a comparison of midspan pressure distributions with experimental data for the NGV and rotor. The case labeled DST base case is from the steady-state, nonlinear simulations used as the base flow for the linearized simulations, and the case labeled nonlinear is the time average of the unsteady nonlinear simulation. Both methods capture the pressure profiles reasonably well.

Time-averaged surface temperatures for the 1–1–1 airfoil count at both hot streak clocking positions are shown at three spanwise locations in Figs. 4–7 for the NGV and the rotor. Figures 4 and 5 show the nonlinear results, and Figs. 6 and 7 show the linearized

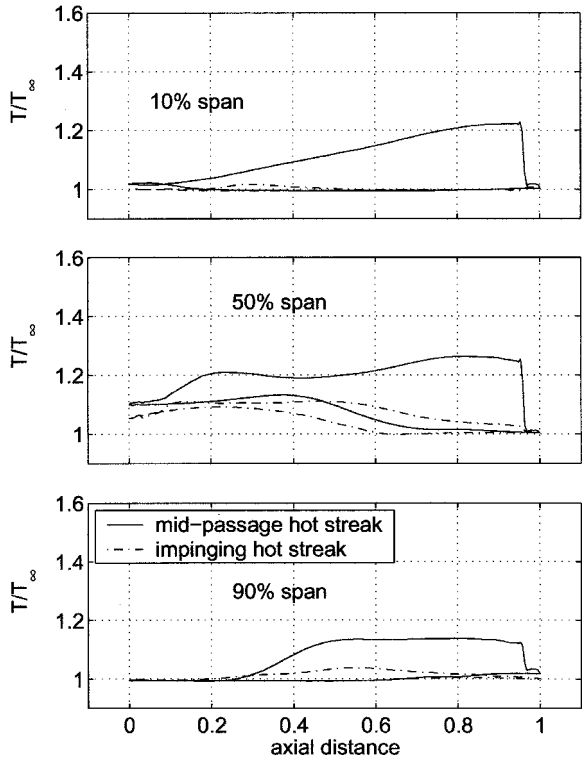

Fig. 5 Time-averaged rotor surface temperature, 1–1–1 blade count, nonlinear simulation.

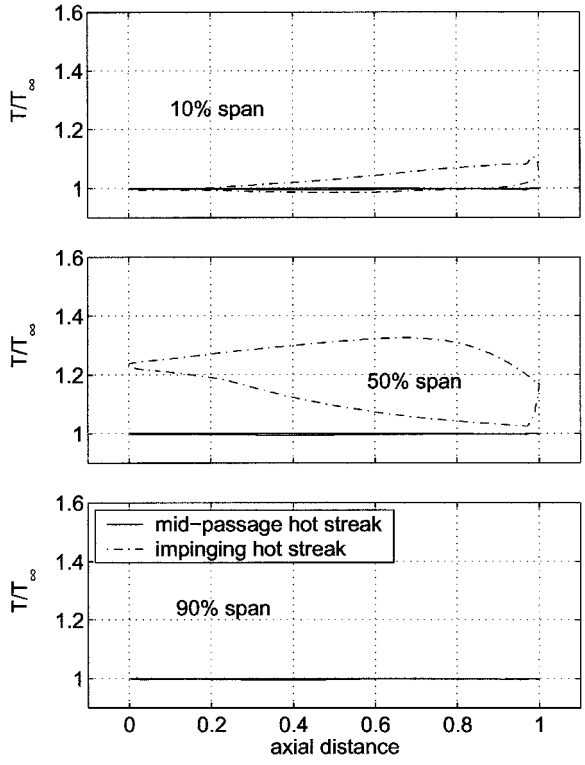

Fig. 6 Time-averaged NGV surface temperature, 1–1–1 blade count, linearized simulation.

results. In the nonlinear results, the NGV shows hotter temperatures for the impinging hot streak case at 10 and 50% span. There is little difference at 90% span because the hot streak is introduced at 40% span. Rotor temperatures are significantly reduced near the hub and tip for the impinging hot streak case, with modest differences near midspan. (The temperatures for the downstream stator, not shown here for brevity, show similar trends.) This illustrates the advantages of hot streak clocking as already discussed.

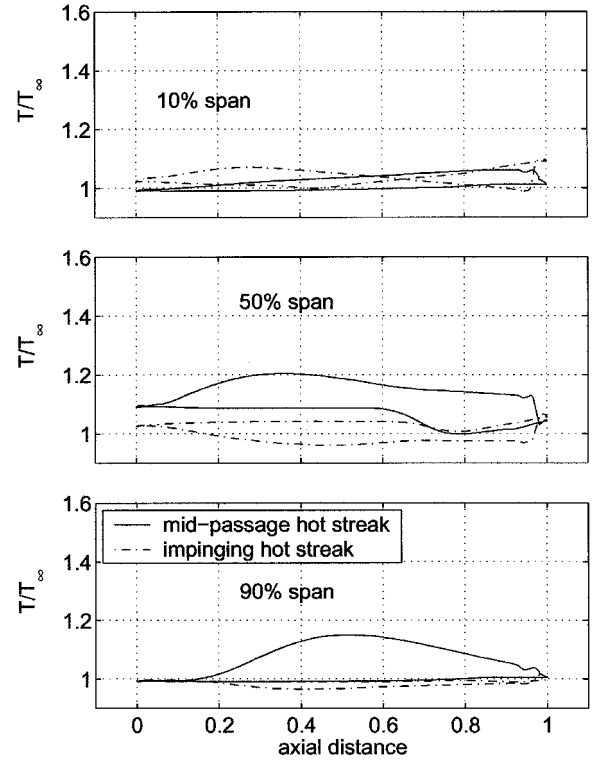

Fig. 7 Time-averaged rotor surface temperature, 1–1–1 blade count, linearized simulation.

At 50% span in the NGV, the linearized technique shows the same qualitative trend as the nonlinear method. The maximum temperature ratio is approximately 1.4 for both cases. The linearized code has second-order spatial accuracy, whereas the nonlinear code has third-order spatial accuracy, and so differences in profile shapes may be due in part to additional dissipation in the linearized code. There is a large difference between the two methods near the hub of the NGV. Because hot streaks in inviscid flow tend not to migrate as they convect through the NGV,[4] the hub heating is primarily due to secondary flow, which is not being captured well in the linearized case. Neither method shows significant heating near the tip.

The linearized case shows the same trends as the nonlinear case in the rotor at 50 and 90% span. Both methods show that clocking the hot streak to impinge on the NGV results in cooler rotor blade surface temperatures. The linearized case underpredicts the magnitude of this effect compared to the nonlinear case.

To investigate these temperature distributions in more detail, the unsteady temperature envelope for the rotor from the nonlinear simulation is shown in Figs. 8. The temperature envelope for the NGV is not shown here because it exhibits little unsteady temperature variation. At 10% span, the impinging hot streak case shows little unsteadiness, whereas the midpassage hot streak case shows a large envelope on the pressure surface. A large amount of unsteadiness is shown on both surfaces for both cases at 50% span. On the suction surface, the maximum temperature is lower for the impinging hot streak case. On the pressure surface, the temperature envelopes are similar, although the maximum temperature is somewhat lower over much of the airfoil for the impinging case. At 90% span, the midpassage hot streak case exhibits more unsteadiness over the aft 65% chord, leading to higher time-averaged temperatures in that region.

Hot Streak Clocking Effects, 3–4–3 Blade Count

Instantaneous temperature contour plots for 40% span sections of the 3–4–3, midpassage and impinging hot streak cases for the nonlinear simulation are shown in Figs. 9 and 10. The hot streak takes on its typical hairpin shape in the rotor passages because the convection speeds are lower near the blade surfaces than at midpassage. The shape of the hot streak in the rotor passage is more

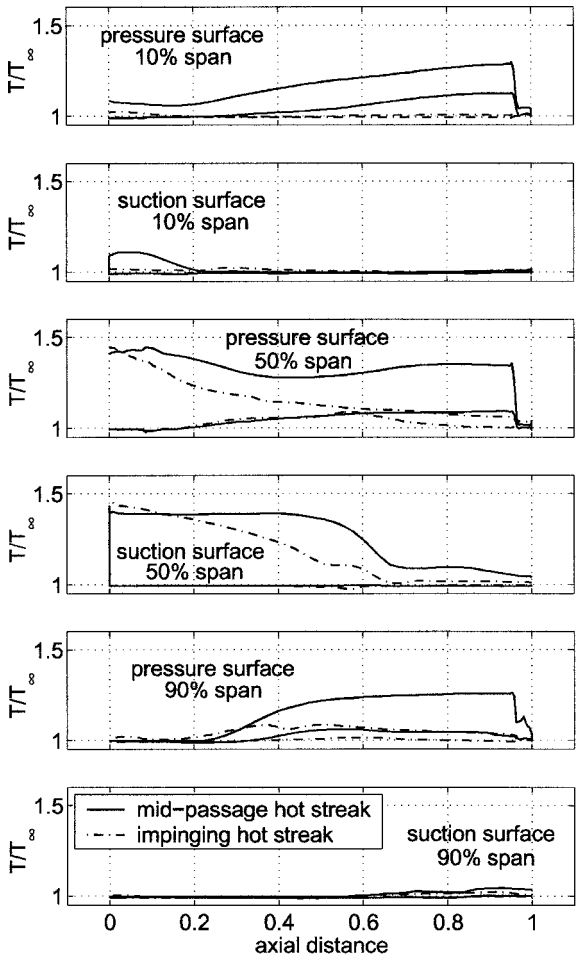

Fig. 8 Rotor surface temperature envelope, 1–1–1 blade count, nonlinear solution.

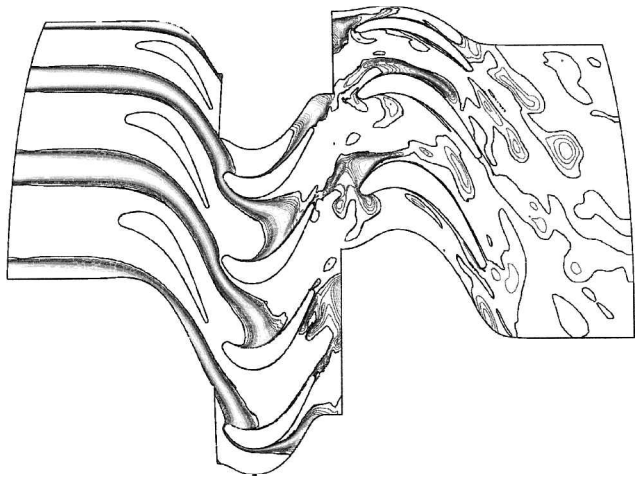

Fig. 9 Instantaneous temperature, 40% span, midpassage hot streak, 3–4–3 blade count, nonlinear simulation, $0 < T/T_\infty < 1.6$.

irregular for the impinging hot streak case because it has interacted with the wake from the NGV.

Time-averaged surface temperatures for the nonlinear 3–4–3 simulation are shown in Figs. 11 and 12. The corresponding linearized cases are shown in Figs. 13 and 14. Here, the trends are once again captured by the linearized simulation at 50 and 90% span.

Comparing Figs. 5 and 12 for the nonlinear case and Figs. 7 and 14 for the linear case shows the differences between the 1–1–1 and 3–4–3 blade-count cases for the rotor. To make the comparison

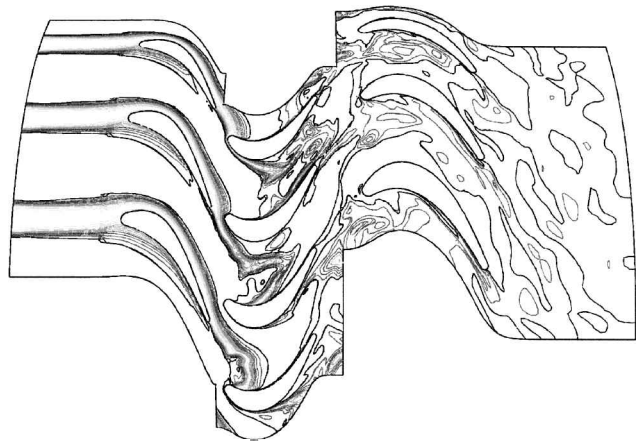

Fig. 10 Instantaneous temperature, 40% span, impinging hot streak, 3–4–3 blade count, nonlinear simulation, $0 < T/T_\infty < 1.6$.

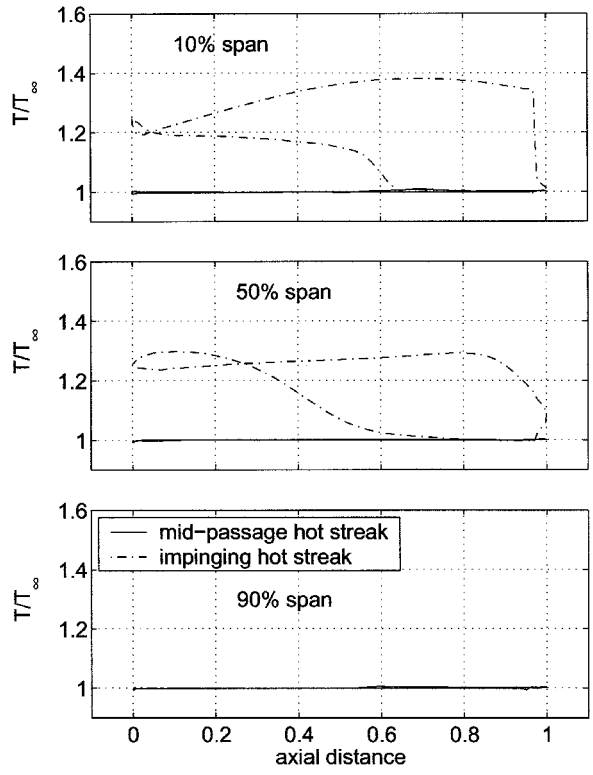

Fig. 11 Time-averaged NGV surface temperature, 3–4–3 blade count, nonlinear simulation.

easier, the results are cross plotted for the midpassage hot streak configuration, shown in Fig. 15. For a given number of hot streaks, it would be expected that more rotor blades would result in lower rotor blade temperatures because the hot streaks are distributed among more rotor passages. This is indeed the observed effect. The differences are particularly large near the endwalls, with relatively small differences at midspan.

To compare the linearized and nonlinear results more easily, results for a sample case, rotor temperatures for the 3–4–3 blade count with midpassage hot streak, have been cross plotted in Fig. 16. The match near the tip is quite good. Although there are discrepancies at midspan, the linearized method still gives a reasonable approximation to blade heating. The results differ at the hub, and this is probably due to differences in secondary flow prediction as mentioned earlier.

Run Times

The simulations in the present study were run on a number of different platforms. Some of the nonlinear Navier–Stokes simulations

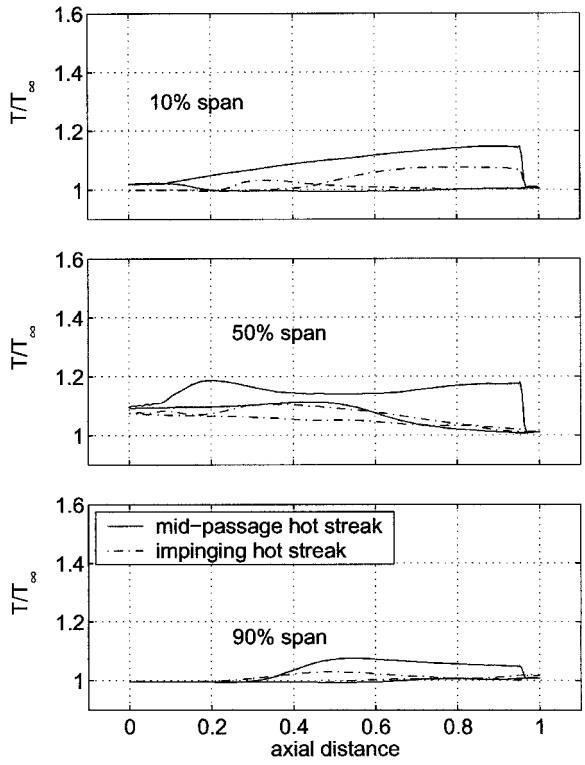

Fig. 12 Time-averaged rotor surface temperature, 3–4–3 blade count, nonlinear simulation.

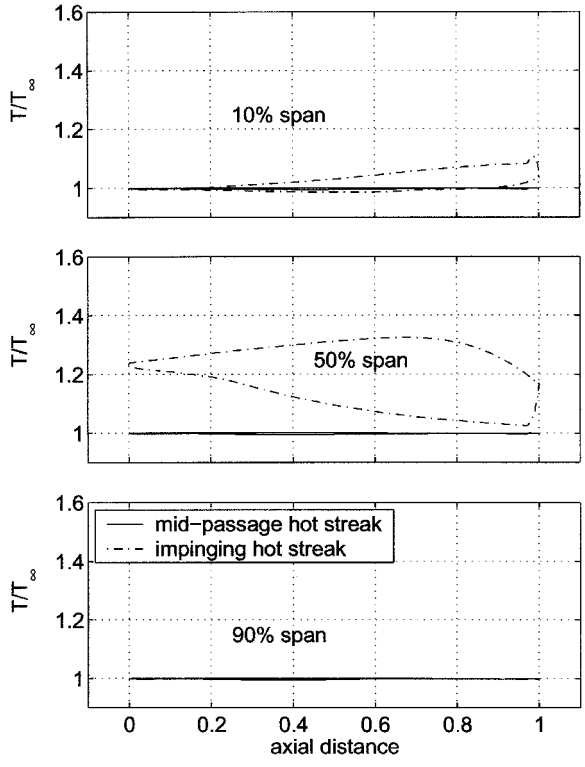

Fig. 13 Time-averaged NGV surface temperature, 3–4–3 blade count, linearized simulation.

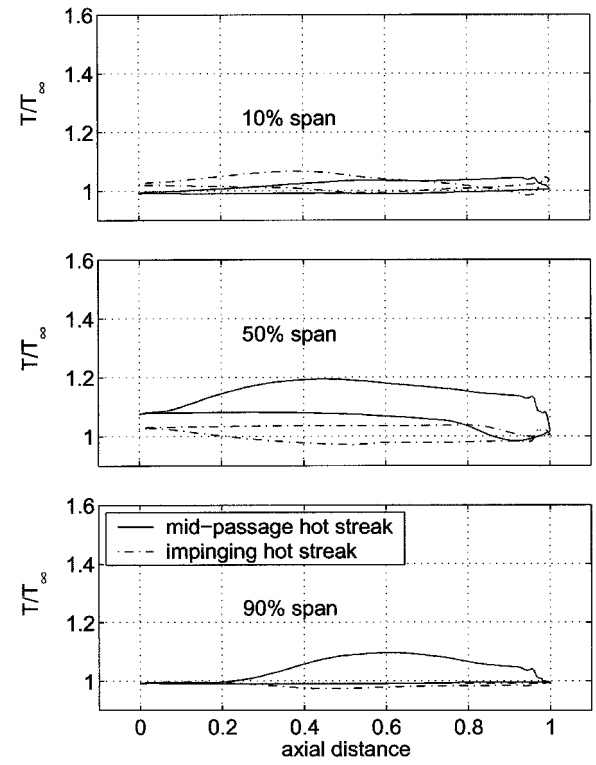

Fig. 14 Time-averaged rotor surface temperature, 3–4–3 blade count, linearized simulation.

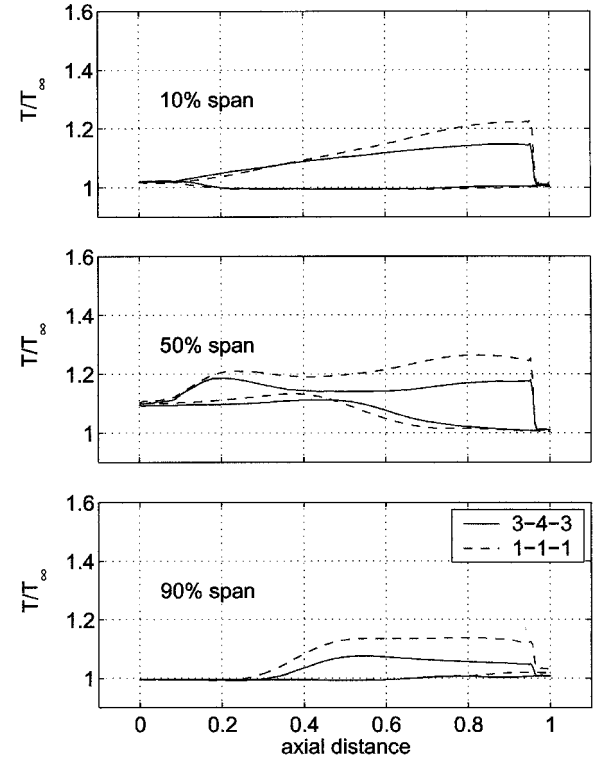

Fig. 15 Rotor surface temperature, midpassage hot streak, nonlinear simulation.

were run on an SGI Origin2000 with 400-MHz R12000 processors. The 1–1–1 blade-count simulations took approximately 550 h on 6 processors, and the 3–4–3 blade-count cases took approximately 950 h on 20 processors.

The linearized cases were run on 733-MHz Pentium III processors. These cases were run for the NGV and rotor only. Once the base flow was computed, the frequency domains were run in parallel, with one frequency per processor. Three frequencies were computed in the present results. This procedure required approximately 100 wall-clock hours for both the base flow and linearized parts.

These run times cannot be compared directly because the linearized base flow simulations were run serially and the frequency-domain simulations were run in parallel, whereas the nonlinear simulations were parallel. To make a reasonable comparison, the wall-clock-processor hours (wall-clock time multiplied by the number of processors used in each corresponding part of the simulation)

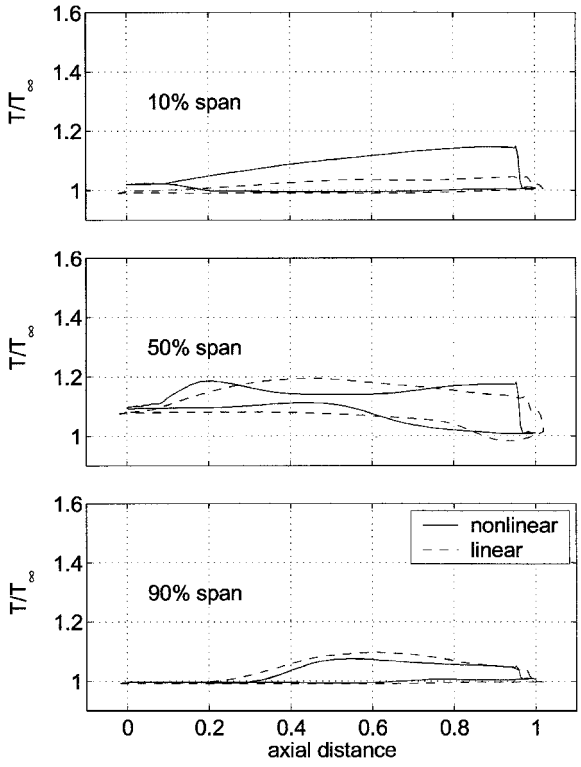

Fig. 16 Rotor surface temperature, midpassage hot streak, 3–4–3 blade count.

per passage will be compared. Based on past experience, the 400-MHz R12000 runs approximately three times as fast as the 733-MHz Pentium III, and so a factor of three will be used.

The nonlinear simulations required approximately 1100 wall-clock-R12000 hours per passage for the 1–1–1 case and approximately 1900 wall-clock-R12000 hours per passage for the 3–4–3 case. When the factor of three is accounted for between the different processors used, the linearized simulations required approximately 70 wall-clock-R12000 hours per passage for all of the simulations. Note that the linearized time is not a function of number of passages when presented in this way because the number of processors scales linearly with the number of passages.

Conclusions

The linearized technique has been shown to capture qualitatively the airfoil surface heating patterns due to hot streak clocking as compared with full unsteady Navier–Stokes simulations. Because the linearized method requires 4–6% of the wall-clock-processor time of the nonlinear simulations, it may be a viable option to improve predictions in the design environment. The advantages are greatest when simulating a large number of passages.

Although the use of reduced blade counts is a reasonable approximation for the reduction of run times for many applications, they result in significant errors in airfoil surface temperature predictions for the hot streak problem. This is true for both the linearized and nonlinear techniques. The errors were shown to be moderate at midspan, but they were large at both the hub and tip endwalls.

Acknowledgments

Part of the funding for this study was provided by Advanced Gas Turbine Systems Research. Computer time for the nonlinear simulations was provided by Boston University and by NASA Advanced Supercomputing at NASA Ames Research Center. The authors would like to thank Brian Mitchell and Scott Hunter for giving us access to the Tacoma code (linearized solver), and to Shane Lennon and Dave Topp for their help. They would also like to thank Matt Goettke for helping to monitor the linearized simulations.

References

[1]Dils, R. R., and Follansbee, P. S., "Use of Thermocouples for Gas Temperature Measurements in Gas Turbine Combustors," 10th Materials Research Symposium on Characterization of High Temperature Vapors and Gases, National Bureau of Standards, Special Publ. 561, Oct. 1979.

[2]Butler, T. L., Sharma, O. P., Joslyn, H. D., and Dring, R. P., "Redistribution of an Inlet Temperature Distortion in an Axial Flow Turbine Stage," *Journal of Propulsion*, Vol. 5, No. 1, 1989, pp. 64–71.

[3]Kerrebrock, J. L., and Mikolajczak, A. A., "Intra-Stator Transport of Rotor Wakes and Its Effect on Compressor Performance," *Journal of Engineering for Power*, Vol. 92, No. 4, 1970, pp. 359–369.

[4]Munk, M., and Prim, R., "On the Multiplicity of Steady Gas Flows Having the Same Streamline Pattern," *Proceedings of the National Academy of Science*, Vol. 33, 1947, pp. 137–141.

[5]Krouthén, B., and Giles, M. B., "Numerical Investigation of Hot Streaks in Turbines," *Journal of Propulsion and Power*, Vol. 6, No. 6, 1990, pp. 769–776.

[6]Dorney, D. J., Davis, R. L., Edwards, D. E., and Madavan, N. K., "Unsteady Analysis of Hot Streak Migration in a Turbine Stage," *Journal of Propulsion and Power*, Vol. 8, No. 2, 1992, pp. 520–529.

[7]Shang, T., and Epstein, A. H., "Analysis of Hot Streak Effects on Turbine Rotor Heat Load," *Journal of Turbomachinery*, Vol. 119, No. 3, 1997, pp. 544–553.

[8]Dorney, D. J., and Gundy-Burlet, K. L., "Hot Streak Clocking Effects in a 1-1/2 Stage Turbine," *Journal of Propulsion and Power*, Vol. 12, No. 3, 1996, pp. 619, 620.

[9]Takahashi, R. K., Ni, R. H., Sharma, O. P., and Staubach, J. B., "Effects of Hot Streak Indexing in a 1-1/2 Stage Turbine," AIAA Paper 96-2796, July 1996.

[10]Gundy-Burlet, K. L., and Dorney, D. J., "Three-Dimensional Simulations of Hot Streak Clocking in a 1-1/2 Stage Turbine," *International Journal of Turbo and Jet Engines*, Vol. 14, No. 3, 1997, pp. 133–144.

[11]Roback, R. J., and Dring, R. P., "Hot Streaks and Phantom Cooling in a Turbine Rotor Passage: Part I—Separate Effects," *Journal of Turbomachinery*, Vol. 115, No. 4, 1993, pp. 657–666.

[12]Orkwis, P. D., Turner, M. G., and Barter, J. W., "Linear Deterministic Source Terms for Hot Streak Simulations," American Society of Mechanical Engineers, ASME Paper 2000-GT-0509, May 2000.

[13]Roe, P. L., "Approximate Riemann Solvers, Parameter Vectors, and Difference Schemes," *Journal of Computational Physics*, Vol. 43, No. 2, 1981, pp. 357, 372.

[14]Baldwin, B. S., and Lomax, H., "Thin Layer Approximation and Algebraic Model for Separated Turbulent Flows," AIAA Paper 78-257, Jan. 1978.

[15]Adamczyk, J. J., "Model Equation for Simulating Flows in Multistage Turbomachinery," American Society of Mechanical Engineers, ASME Paper 85-GT-226, March 1985.

[16]Sondak, D. L., Dorney, D. J., and Davis, R. L., "Modeling Turbomachinery Unsteadiness with Lumped Deterministic Stresses," AIAA Paper 96-2570, July 1996.

[17]Busby, J., Sondak, D. L., Staubach, B., and Davis, R., "Deterministic Stress Modeling of Hot Gas Segregation in a Turbine," *Journal of Turbomachinery*, Vol. 122, No. 1, 2000, pp. 62–67.

[18]Holmes, D. G., Mitchell, B. E., and Lorence, C. B., "Three Dimensional Linearized Navier–Stokes Calculations for Flutter and Forced Response," *Unsteady Aerodynamics and Aeroelasticity of Turbomachines*, edited by T. H. Fransson, Kluwer Academic, Norwell, MA, 1997, pp. 221–224.

[19]Dring, R. P., Blair, M. F., Joslyn, H. D., Power, G. D., and Verdon, J. M., "The Effects of Inlet Turbulence and Rotor/Stator Interactions on the Aerodynamics and Heat Transfer of a Large-Scale Rotating Turbine Model. I—Final Report," NASA CR 4079, Contract NAS3-23717, May 1986.